

Production of picosecond, kilojoule, petawatt laser pulses via Raman amplification of nanosecond pulses

R.M.G.M. Trines,^{1,*} F. Fiúza,² R. Bingham,^{1,†} R.A.
Fonseca,^{2,‡} L.O. Silva,² R.A. Cairns,³ and P.A. Norreys^{1,§}

¹*Central Laser Facility, STFC Rutherford Appleton Laboratory,
Harwell Science and Innovation Campus,
Didcot, Oxon, OX11 0QX, United Kingdom*

²*GoLP/Instituto de Plasmas e Fusão Nuclear - Laboratório Associado,
Instituto Superior Técnico, 1049-001 Lisbon, Portugal*

³*University of St Andrews, St Andrews, Fife KY16 9AJ, United Kingdom*

(Dated: November 10, 2018)

Abstract

Raman amplification in plasma has been promoted as a means of compressing picosecond optical laser pulses to femtosecond duration to explore the intensity frontier. Here we show for the first time that it can be used, with equal success, to compress laser pulses from nanosecond to picosecond duration. Simulations show up to 60% energy transfer from pump to probe pulses, implying that multi-kilojoule ultra-violet petawatt laser pulses can be produced using this scheme. This has important consequences for the demonstration of fast-ignition inertial confinement fusion.

PACS numbers: 52.38.-r, 42.65.Re, 52.38.Bv, 52.38.Hb

The demonstration of fast-ignition (FI) inertial confinement fusion (ICF) involves two phases: the compression of deuterium-tritium fuel to high density and the formation of a hot spot region on the side of the fuel at peak compression via the stopping of energetic (1–3 MeV) electrons generated by an intense picosecond laser pulse. [1, 2]. Even with the deployment of different magnetic collimation concepts, between 40 kJ - 100 kJ of laser energy needs to be delivered within 16 ps to produce an electron beam with the required properties [1, 3–6]. High-energy petawatt beams of 1-10 picosecond duration are difficult to generate using conventional solid-state laser systems.

Previous studies of Raman amplification have concentrated on reaching the intensity frontier, which requires ultra-short pulses in the femtosecond regime [7–13]. Here we present novel particle-in-cell simulations, supported by analytic theory, that confirm that Raman amplification of high-energy nanosecond pulses in plasma can generate efficient petawatt peak power pulses of picosecond duration with high conversion efficiency (up to 60%). The scheme can easily be scaled from ω_0 to $3\omega_0$ pulses: only the plasma density needs to be adjusted such that the ratio ω_0/ω_p remains fixed (where $\omega_0 = 2\pi c/\lambda_0$ is the laser frequency, λ_0 its wave length, $\omega_p = \sqrt{e^2 n_0/(\varepsilon_0 m_e)}$ is the plasma frequency, and n_0 is the plasma electron density, while e , ε_0 and m_e have their usual meaning). This scheme provides a new route to explore the full parameter space for the realisation of the fast ignition inertial confinement fusion concept in the laboratory. This work also opens up a wide range of other high energy density physics research applications, including monochromatic K_α x-ray [14], proton beam [15] and Compton radiography of dense plasmas [16], among many others.

Raman amplification in plasma (characteristic plasma frequency ω_p) works as follows [7, 8]. A long pump laser beam (frequency ω_0 , wave number k_0) and a counter-propagating short probe pulse (frequency $\omega_0 - \omega_p$, wave number $\omega_p/c - k_0$) interact via a longitudinal plasma wave (frequency ω_p , wave number $2k_0 - \omega_p/c$) via the process known as stimulated Raman backscattering [17]. This causes a large fraction of the energy of the long pump pulse to be transferred to the short probe pulse. Because the amplified probe is normally up to 1000 times shorter than the pump, its final power can be hundreds of times higher than that of the pump beam.

Raman amplification of ultra-short (~ 25 fs) pulses at high intensities was the subject of an extensive recent investigation [12]. In the case of FI in ICF, however, the compression of long (nanosecond) pump beams to medium (picosecond) duration is needed. This cannot be

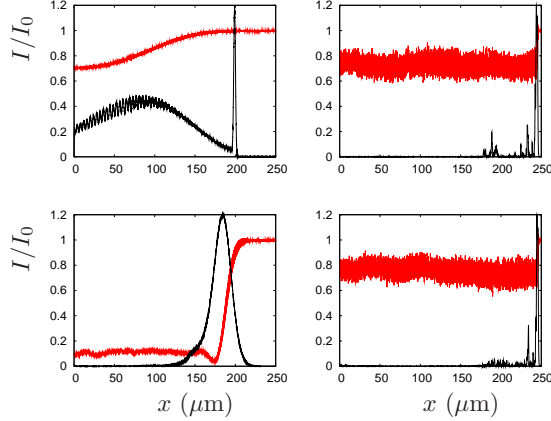


Figure 1: Effects of pump intensity of growth of long and short probes. Shown are the relative intensities of pump (red) and probe (black) versus longitudinal coordinate in μm . Top row: 50 fs probe and pump with $a_0 = 0.01, 0.1$ respectively. The less intense pump causes the short probe to stretch, while the more intense pump causes the probe to remain short. Bottom row: Same as before, but with 500 fs probe. At low pump intensity the probe remains long, while at higher pump intensity the probe is shortened.

done by simply extending the scheme of Ref. [12] (pump intensities of $10^{14} - 10^{15} \text{ W/cm}^2$) to longer pump pulses because of the increasing influence of pump and probe instabilities, probe saturation and probe shortening at longer interaction lengths. However, it follows from the self-similar theory of Raman amplification developed by Malkin, Shvets and Fisch [8] that ns-to-ps compression can be accomplished by reducing the intensities of pump and probe. Although the self-similar theory has been used to predict the self-contraction of the probe [8, 9, 18–20], it has not been used before to increase the final probe duration. We introduce the dimensionless pulse amplitude $a \equiv 8.55 \times 10^{-10} \sqrt{g} \sqrt{I \lambda^2 [\text{Wcm}^{-2} \mu\text{m}^2]}$, where I and λ denote the peak intensity and wave length of the laser beam (pump or probe) under consideration and $g = 1$ ($g = 1/2$) denotes linear (circular) polarisation, and write a_0 (a_1) to denote the amplitude of the pump (probe) pulse. Following Malkin *et al.* [8], we find that the probe duration after amplification is given by

$$t_{\text{probe}} = 2g\xi_M^2 / (\omega_0 \omega_p a_0^2 t_{\text{pump}}) \quad (1)$$

where ξ_M is a constant of the self-similar interaction, $\xi_M \sim 5$ for a 1 ps probe at 351 nm and $10^{13} \text{ W cm}^{-2}$, and increases by ~ 1 when the intensity decreases by an order of magnitude. Thus, the probe duration can be increased by keeping the pump intensity low, even for long

pump pulses. If one fixes $\omega_0/\omega_p = 20$ and $t_{\text{pump}}/t_{\text{probe}} = 1000$ as in [12], then the pump intensity needed to obtain a certain optimal probe duration is given by:

$$I_{\text{pump}} = 3.9 \times 10^{11} / (t_{\text{probe}}[\text{ps}])^2 \text{ [W/cm}^2\text{]}, \quad (2)$$

independent of pump laser wave length. As an example, producing a 2 ps probe from a 2 ns pump requires an intensity of $1.0 \times 10^{11} \text{ W cm}^{-2}$.

To illustrate this, Figure 1 shows the results of four 1-D particle-in-cell simulations (using the code XOOPIIC [21]) where the pump intensity is either high or low, and the initial probe duration is either long or short. It is found that a low pump intensity leads to a long final probe, while a high pump intensity leads to a short final probe, independent of the initial probe duration.

Limits on the applicability of the self-similar theory are posed by the pump intensity, compression ratio and the frequency ratio ω_0/ω_p . The pump intensity should not exceed the value given by (2) by much, and the compression should not be (much) larger than 1000, both to avoid damage by instabilities. Although increasing ω_0/ω_p will increase the duration of the probe, it will also facilitate wave breaking of the Langmuir wave that couples pump and probe, disrupting the amplification process [8]; using $\omega_0/\omega_p \leq 20$ is recommended to prevent this.

Lowering the pump intensity will increase the duration of the amplified probe even further. This has been explored in a series of full particle-in-cell (PIC) numerical simulations using the codes XOOPIIC and OSIRIS [22]. In all simulations, the central pump wave length was 351 nm, the plasma density was $2.3 \times 10^{19} \text{ cm}^{-3}$ ($\omega_0/\omega_p = 20$), and the plasma was initially cold with static ions. In order to infer the effects of the ion motion in the amplification of long pulses, simulation (III) below was repeated with mobile ions (simulation III'). The amplified pulse achieved similar levels of amplification and a good final pulse shape, justifying the use of static ions in the other simulations.

The summary of our simulation results is shown in Table I. Overall, the final probe duration is found to increase with decreasing pump amplitude, and to decrease with increasing pump duration. For simulations (II)-(V), the efficiency is 40-60% and the self-similar parameter ξ_M ranges from 6 to 9, in reasonable agreement with the theoretical prediction $5 < \xi_M < 7$. The poor efficiency in (I) is caused by the combination of high pump intensity and long interaction length, triggering premature pump RBS and probe saturation. The

	I	II	III	III'	IV	V	VI
a_0	0.0044	0.003	0.0016	0.0016	0.001	0.001	0.00056
a_1	0.0044	0.003	0.0044	0.0044	0.003	0.001	0.00056
t_{pu} (ps)	100	133	100	100	67	133	133
t_{pr} (fs)	65	28	230	330	400	283	2180
Eff.(%)	20	39	50	40	60	44	7
ξ_M	14.2	7.0	8.9	10.6	6.2	7.3	11.5

Table I: Summary of our simulation results. In each simulation, $\lambda_0 = 351$ nm and $\omega_0/\omega_p = 20$ were used. For each simulation, the initial pump (a_0) and probe (a_1) amplitudes, initial pump (t_{pu}) and final probe (t_{pr}) duration, and energy transfer efficiency are given, as well as $\xi_M = (a_0^2 \omega_0 \omega_p t_{\text{pu}} t_{\text{pr}})^{1/2}$, to verify compliance with the self-similar theory. Simulation (III') is similar to (III), only using mobile ions.

poor efficiency in (VI) is caused by the long start-up time (see below) resulting from the low pump and probe intensities. These simulations also exhibit a relatively high value for ξ_M , showing that the probe has not yet fully entered the self-similar regime (VI) or has already left it (I).

The amplification of the probe may be affected by a number of instabilities: Raman forward scattering, modulational instability, filamentation, and parasitic RBS of the pump before it meets the probe. Full-scale multi-dimensional PIC simulations are needed to investigate such instabilities properly, see e.g. Ref. [12], but this may not be practical given the interaction distances involved (e.g. 150 mm for an 1 ns pump). Nevertheless, the impact of the filamentation, modulational and Raman forward scattering instabilities on the growing probe can be estimated as follows. From Ref. [8], we find that the characteristic growth times for these instabilities are given by $t_{\text{fw}} \propto 1/(a_0 \omega_p^{3/2})$ and $t_{\text{md}} \propto 1/(a_0^{4/3} \omega_p)$. For a fixed ω_0 , ω_p and compression ratio, e.g. $t_{\text{probe}} = t_{\text{pump}}/1000$, we have $t_{\text{probe}} t_{\text{pump}} \propto t_{\text{pump}}^2 \propto 1/a_0^2$. Then $t_{\text{pump}}/t_{\text{fw}}$ does not depend on a_0 , while $t_{\text{pump}}/t_{\text{md}} \propto a_0^{1/3}$, i.e. this ratio improves for decreasing a_0 . For the filamentation instability in the short-pulse limit, Max *et al.* [23] or Bingham and Lashmore-Davies [24] provide a growth rate of $\gamma = (a_0^2/8)(\omega_p^2/\omega_0)$, so $t_{\text{fil}} \propto 1/a_0^2$ and $t_{\text{pump}}/t_{\text{fil}} \propto a_0$, once again improving for decreasing a_0 . In short, Raman amplification of long pulses at low intensities suffers less from damaging instabilities than it does for short

pulses at high intensities.

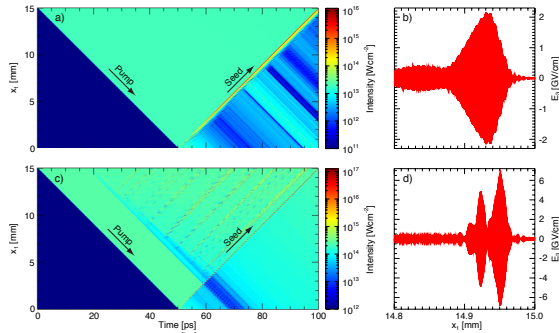


Figure 2: Raman amplification of a 100 ps pump to obtain a ~ 200 fs probe, for a pump wave length of 351 nm. (a) Intensity versus position and time for the entire pump-probe interaction, for a pump intensity of 2.7×10^{13} W/cm², obtained using Eq. (2). For this intensity, the pump propagation is stable with hardly any precursors to the relatively long probe, while the pump is efficiently depleted. (b) Transverse electric field of the final probe for the intensity under (a). (c) As (a), but for a pump intensity of 2×10^{14} W/cm². Premature pump RBS generates precursors to the probe pulse, which is much shorter while the pump depletion is less. (d) Transverse electric field of the final probe for the intensity under (c).

Simulations of the entire plasma column have been conducted, using OSIRIS, to study the stability of a 100 ps pump pulse as it traverses a 15 mm plasma column before it meets the probe. Figure 2 shows the results from simulations (I) and (III) in Table I, where (III) has a pump intensity of 2.7×10^{13} W/cm², obtained using Eq. (2), while (I) has a much higher intensity of 2×10^{14} W/cm², all other parameters identical. For the lower intensity, both pump propagation and probe amplification are stable, and a smooth probe is obtained without precursors. For the higher intensity, the pump suffers from parasitic instabilities, mostly premature RBS, leading to probe precursors, and the probe is shorter while its envelope is less smooth, which is partly caused by the probe taking on the characteristic multi-period π -pulse shape. This emphasises the importance of keeping the intensity at or below the value predicted by Eq. (2), when the Raman amplification of a long pump is required.

One issue that is not immediately obvious from the self-similar theory is the existence of a “start-up period” for Raman amplification of low-intensity pulses. The simulations show that when both pump and probe amplitudes are below $a_0 = 0.01$ ($\sim 10^{14}$ W/cm²)

for a $\sim 1 \mu\text{m}$ pump wave length), the pump and probe need to interact over several mm before the probe amplification starts in earnest. For a 2 ps initial probe duration, this ranges from less than 2 mm for $a_0 = a_1 = 0.001$ and 10 mm for $a_0 = a_1 = 0.000562$ to 20 mm for $a_0 = a_1 = 0.0003$. This follows from the fact that the initial probe amplitude and duration for the ideal self-similar solution are related as $t_{\text{probe}} \approx 4 \times 10^{-15}/a_1$ ($\lambda_0 = 351 \text{ nm}$, $\omega_0/\omega_p = 20$). Thus, a 2 ps initial probe duration ideally requires $a_1 = 0.002$ initially. In our simulations, however, a_1 is well below that value and the actual probe requires an increasing amount of time to evolve into a self-similar probe for decreasing a_1 . Hence the start-up period, whose length also depends on the pump intensity. This effect can be mitigated by increasing the initial probe intensity and/or duration, thus ensuring that the start-up period remains a limited fraction of the pump duration and the overall efficiency remains reasonable even for very low pump intensities.

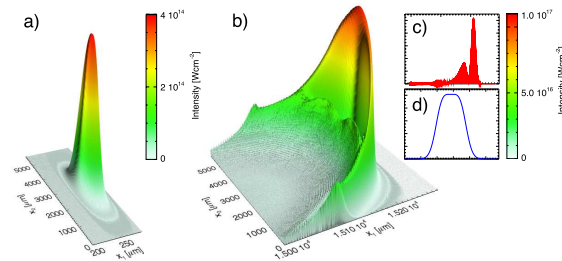


Figure 3: Raman amplification of a 100 ps long pump to obtain a $\sim 150 \text{ fs}$, mm wide, 2 PW probe, for a wave length of 351 nm. (a) Initial and (b) final intensity profile of the probe pulse after amplification in a 1.5 cm plasma column. Insets show central lineouts of the amplified pulse in the (c) longitudinal and (d) transverse directions.

In order to study the stability of the process in multiple dimensions, where transverse instabilities can come into play, we have performed a 2D OSIRIS simulation using the parameters of simulation (III) and a probe spot FWHM of 1.2 mm. This relatively wide probe pulse is efficiently amplified to a peak intensity of 10^{17} Wcm^{-2} , corresponding to a final power of $\sim 1.5 \text{ PW}$ (Fig. 3). As predicted for these optimized parameters, transverse instabilities are controlled and the amplified pulse retains a smooth envelope. The bowed shape of the amplified pulse is similar to the shape observed for ultrashort pulses [12], and does not influence the amplification process. While the final pulse power significantly exceeds the critical power for self-focusing, $P_c = 17(\omega_0/\omega_p)^2 \text{ GW} = 6.8 \text{ TW}$ [25], no significant self-

focusing occurs during the interaction, which can be explained as follows. The spot radius R of a self-focusing laser pulse in plasma is described by $R = R_0 \sqrt{1 - z^2/z_0^2}$, where R_0 is the minimum spot radius in vacuum and $z_0 = z_R/\sqrt{P/P_c - 1}$ is the typical distance for self-focusing, with $z_R = \pi R_0^2/\lambda$ being the Rayleigh length and P the laser power. For a 1.5 PW laser pulse with $R_0 = 1$ mm and $\lambda = 351$ nm, $z_0 = 63$ cm, significantly exceeding the typical amplification distances involved (1.5 – 2 cm). Higher powers require larger spot sizes, since the intensity I is fixed by the probe duration and compression ratio; this leads to $z_R \propto P/I \propto P$ and $z_0 \propto \sqrt{P}$. Thus, the influence of self-focusing decreases for increasing probe power.

In the above 2-D simulation, a 2.7×10^{13} W/cm², 100 ps pump has been used to obtain a ~ 150 fs probe with a smooth envelope. In simulation (IV), a $\sim 10^{13}$ W/cm², 67 ps pump has been used to obtain a 0.4 ps probe. Furthermore, it was shown in ref. [12] that a 25 ps pump at 10^{15} W/cm² (800 nm wave length) can be compressed to about 25 fs while probe modulation and RFS remain at an acceptable level. Extrapolating these cases via the self-similar theory, we predict that a 2 ps probe can be obtained using a 2 ns pump at an intensity of $(0.7 - 1.5) \times 10^{11}$ W/cm², in good agreement with the value of 1.0×10^{11} W/cm² predicted by Eq. (2). Assuming the pump beam contains 10 kJ in 2 ns, the pump power will be 5 TW, so a 50 cm² cross section is needed for the interaction. Such energetic pump beams can be obtained at e.g. the National Ignition Facility [26], the Omega EP laser system at the Laboratory for Laser Energetics in Rochester [27, 28], and the Laser Mégajoule project [29].

In summary, we have investigated the Raman amplification and compression of nanosecond laser pulses to picosecond duration, exploiting the self-similar properties of the process. We have shown that, for a constant pump-to-probe compression ratio, the optimal pump and probe durations will increase for decreasing pump intensity. In addition, we have shown that the relative importance of undesirable instabilities remains the same (pump RBS, probe RFS) or even decreases (modulational and filamentation instabilities) with decreasing pump intensity. Energy transfer efficiencies of up to 60% have been found. Thus, Raman amplification in plasma can be used to generate picosecond pulses of moderate intensity but large total energy. This has important consequences for a wide range of applications in high energy density physics, particularly fast-ignition ICF and x-ray and proton radiographic diagnosis of dense plasmas. Most importantly, our approach provides a potential route to the

full-scale demonstration of fast ignition inertial confinement fusion using existing facilities.

Work supported by STFC's Central Laser Facility and Centre for Fundamental Physics, by EPSRC through grant EP/G04239X/1, by the European Research Council (ERC-2010-AdG Grant 267841), and by FCT (Portugal) grants PTDC/FIS/111720/2009 and SFRH/BD/38952/2007. We thank C. Joshi, N. Fisch and R. Kirkwood for stimulating discussions, N. Loureiro for the moving-window antenna in OSIRIS, UC Berkeley for the use of XOOPIIC and the OSIRIS consortium for the use of OSIRIS. We acknowledge the assistance of HPC resources (Tier-0) provided by PRACE on Jugene (Germany). Simulations were performed on the Scarf-Lexicon Cluster (STFC RAL), the IST Cluster (IST Lisbon), the Hoffman cluster (UCLA) and the Jugene supercomputer (Germany).

* also at Lancaster University, Lancaster, UK

† also at University of Strathclyde, Glasgow, UK

‡ also at DCTI/ISCTE Lisbon University Institute, 1649-026 Lisbon, Portugal

§ also at Imperial College London, London, UK

- [1] S. Atzeni *et al.*, Phys. Plasmas **15**, 056311 (2008).
- [2] J. Honrubia and J. Meyer-ter-Vehn, Plasma Phys. Control. Fusion **51** 014008 (2009).
- [3] A.J. Kemp, Y. Sentoku and M. Tabak, Phys. Rev. E **79**, 066406 (2009).
- [4] P.A. Norreys *et al.*, Nucl. Fusion **49**, 104023 (2009).
- [5] M.S. Wei *et al.*, Phys. Plasmas **15**, 083101 (2008).
- [6] M. Tabak *et al.*, Phys. Plasmas, **1**, 1626 (1994).
- [7] G. Shvets *et al.*, Phys. Rev. Lett. **81**, 4879-4882 (1998).
- [8] V.M. Malkin *et al.*, Phys. Rev. Lett. **82**, 4448-4451 (1999).
- [9] V.M. Malkin and N.J. Fisch, Phys. Plasmas **12**, 044507 (2005).
- [10] J. Ren *et al.*, Nature Physics **3**, 732-736 (2007).
- [11] Y. Ping *et al.*, Phys. Plasmas **16**, 123113 (2009).
- [12] R.M.G.M. Trines *et al.*, Nature Physics **7**, 87 (2011).
- [13] R.K. Kirkwood *et al.*, Phys. Plasmas **18**, 056311 (2011).
- [14] H.-S. Park *et al.*, Phys. Plasmas **13**, 056309 (2006).
- [15] M. Borghesi *et al.*, Phys. Plasmas **9**, 2214 (2002).

- [16] R. Tommasini *et al.*, Rev. Sci. Instrum. **79**, 10E901 (2008).
- [17] D.W. Forslund, J.M. Kindel and E.L. Lindman, Phys. Fluids **18**, 1002-1016 (1975).
- [18] J. Kim, H.J. Lee, H. Suk and I.S. Ko, Phys. Lett. A **314**, 464 (2003).
- [19] D.S. Clark and N.J. Fisch, Phys. Plasmas **10**, 4837 (2003).
- [20] D.S. Clark and N.J. Fisch, Phys. Plasmas **10**, 4848 (2003).
- [21] J.P. Verboncoeur, A.B. Langdon and N.T. Gladd, Comp. Phys. Comm. **87**, 199-211 (1995).
- [22] R.A. Fonseca, L.O. Silva, R.G. Hemker, *et al.*, Lect. Not. Comp. Sci. **2331**, 342-351 (2002).
- [23] C.E. Max, J. Arons and A.B. Langdon, Phys. Rev. Lett. **33**, 209-212 (1974).
- [24] R. Bingham and C.N. Lashmore-Davies, Nuclear fusion **16**, 67 (1976).
- [25] P. Sprangle, C.-M. Tang, and E. Esarey, IEEE Trans. Plas. Sci. **15**, 145-153 (1987).
- [26] E.I. Moses, J. Phys. Conf. Ser. **112**, 012003 (2008).
- [27] T.R. Boehly *et al.*, Opt. Commun. **133**, 495 (1997).
- [28] L.J. Waxer *et al.*, Opt. Photon. News **16**, 30 (2005).
- [29] N. Fleurot, C. Cavailler and J.L. Bourgade, Fusion Engineering and Design **74**, 147 (2005).